The global structure of periodic solutions to a suspension bridge mechanical model

P.J. McKenna * K.S. Moore †

June 10, 2002

Abstract

We study two systems of nonlinearly coupled ordinary differential equations that govern the vertical and torsional motions of a cross section of a suspension bridge. We observe numerically that the structure of the set of periodic solutions changes considerably when we smooth the nonlinear terms. The smoothed nonlinearities describe the force that we wish to model more realistically and the resulting periodic solutions more accurately replicate the phenomena observed at the Tacoma Narrows Bridge on the day of its collapse. The main conclusion is that purely vertical periodic forcing can result in subharmonic primarily torsional motion.

Keywords: torsional oscillations, coupled oscillations, suspension bridge
AMS subject classification: 34C15, 34C25

1 Introduction

As was made abundantly clear by the opening and rapid closing of the Millennium Bridge in London in 2000 [1], the science of the dynamics of suspension bridges still has many large gaps. Although near-equilibrium motions

*Department of Mathematics, University of Connecticut, Storrs, CT 06269-3009. *email: mckenna@math.uconn.edu*

†Department of Mathematics, University of Michigan, Ann Arbor, MI 48109-1109. *email:ksmoore@umich.edu*

are fairly well understood, as soon as the motions deviate from the equilibrium by several feet, unpredictable things happen. When these unwanted oscillations occur, the engineer usually has only two remedies: adding extra damping or changing the physical constants by increasing the stiffness.

This paper continues a series of papers in which we model the dynamics of large nonlinearly suspended objects with two degrees of freedom, in the torsional and vertical direction. The reader will note that it doesn't claim to apply directly to the Millennium Bridge since those oscillations had a pronounced lateral component. However, the conclusions we reach presumably still have some relevance to those unwanted oscillations.

In [7], the first author considered a horizontal cross section of the center span of a suspension bridge and proposed ordinary differential equation (ODE) models for the coupled vertical and torsional motions of the cross section. In [10], [11], the second author extended these models to include spatial dependence and studied the coupled vertical and torsional motions along the entire length of the span.

In both cases, using physical constants from the engineers' reports of the 1940 collapse of the Tacoma Narrows bridge, we were able to numerically replicate one of the most fascinating and previously unexplained phenomena observed at Tacoma Narrows, namely the rapid transition from the bridge's usual vertical motion to the destructive torsional oscillation that preceded the collapse. We found that even with *tiny* torsional forcing or initial displacement, large vertical motion could rapidly induce a change to large torsional motion.

More specifically, we found that if the vertical motion was sufficiently large to induce brief slackening of the cables that suspend the roadbed, the result was a rapid transition to large amplitude torsional motion. Eyewitnesses at the collapse observed that the vertical acceleration that preceded the change to torsional motion exceeded gravitational acceleration [2], thus we believe that such slackening did occur at Tacoma Narrows on the day of the collapse.

Despite the physical and mathematical appeal of the phenomenon described above, the result had several shortcomings, which are outlined in [9]. Most notably, the range of parameters over which the transition from vertical to torsional motion was observed was physically unreasonable. Also, the treatment of the restoring force due to the cables was oversimplified; the nonlinear terms in the model describe a cable that behaves perfectly linearly

when it is in tension (regardless of the size of the oscillation) and that can completely lose tension. Finally, in order to induce the transition from vertical to torsional motion, it was necessary to impose small torsional forcing. As this type of type of force had been observed in wind tunnel experiments, this seemed justified, [12].

On the other hand, although the Tacoma Narrows Bridge oscillated vertically regularly during its four month life, the torsional oscillations that preceded the collapse were never observed until the day of the collapse. Thus there is considerable historical evidence for the presence of periodic vertical forcing, but no evidence of the type of periodic torsional forcing that we imposed in [7], [8], [10], [11].

In [9], the authors found that with a slight modification to the existing model, they could address the shortcomings described above and find the desired torsional response to near-equilibrium vertical forcing. More specifically, they smoothed the nonlinear terms in the original model so that the smoothed nonlinearities more accurately capture the qualitative behavior of the restoring force exerted by the cables, namely, linear restoring force near equilibrium, superlinear force for large oscillations when the cables are in tension, and small nonzero resistance to compression.

The authors solved initial value problems for the smoothed system under various physical assumptions and found that the periodic response of the smoothed system differed dramatically from the solutions to the original system. Most notably, in the smoothed problem, small vertical oscillations alone were sufficient to induce large torsional motion, even with zero torsional forcing, [9]. (In the original system, unreasonably large vertical motion and small torsional forcing were required to induce the transition to torsional motion, [7], [10], [11].)

In this paper, we present a systematic study of the structure of the set of periodic solutions to the smoothed problem and contrast it with that of the original system proposed in [7]. In section 2, we describe both the original piecewise linear model and the smoothed system that govern the vertical and torsional motion of a cross section of a suspension bridge. In section 3, we discuss solutions to the piecewise linear model and in section 4, we discuss the bifurcation and stability properties of periodic solutions to the smoothed problem. We see that this slight modification gives rise to rich and surprising results, including the following.

- We are able to replicate the phenomenon observed in [9]; i.e., small vertical oscillations are sufficient to induce large torsional motion, even with zero torsional forcing. Moreover, we isolate the range of parameters over which this phenomenon occurs.
- The periodic solutions to the smoothed system possess surprising stability properties, including unstable small amplitude solutions which give rise to stable large amplitude solutions.
- More complicated bifurcation curves arise for the smoothed problem as we vary the amplitudes and frequencies of the external forcing terms.

Finally, in section 5, we describe open problems and future directions for this work.

2 The Models

We view the main span of the bridge as a beam of length L and width $2l$ suspended by cables, see figure 1. Consider the cross section located at position $x \in (0, L)$. In this paper we ignore the dependence on the spatial variable x; this dependence is studied in [10], [11]. The forces that we will model are the cables suspending the cross section, damping, gravity, and external forcing, which we describe in section 2.3. We will consider two different models for the force due to the cables: a one sided Hooke's law and exponential force.

2.1 Piecewise linear cable force

In this section we will assume, as we did in [7], [10], [11], that the cables resist elongation according to Hooke's law, but do not resist compression. Let $z(t)$ be the downward displacement of the center of the cross section from the unloaded state at time t and let $\theta(t)$ be the angular deflection from horizontal. Observe that the stretch in one cable is given by $z - l\sin\theta$ and the stretch in the other cable is $z + l\sin\theta$, see figure 1.

Then the force exerted by the right hand cable is

$$f = \begin{cases} -K(z - l\sin\theta) & z - l\sin\theta \geq 0 \\ 0 & z - l\sin\theta < 0 \end{cases} = -K(z - l\sin\theta)^+$$

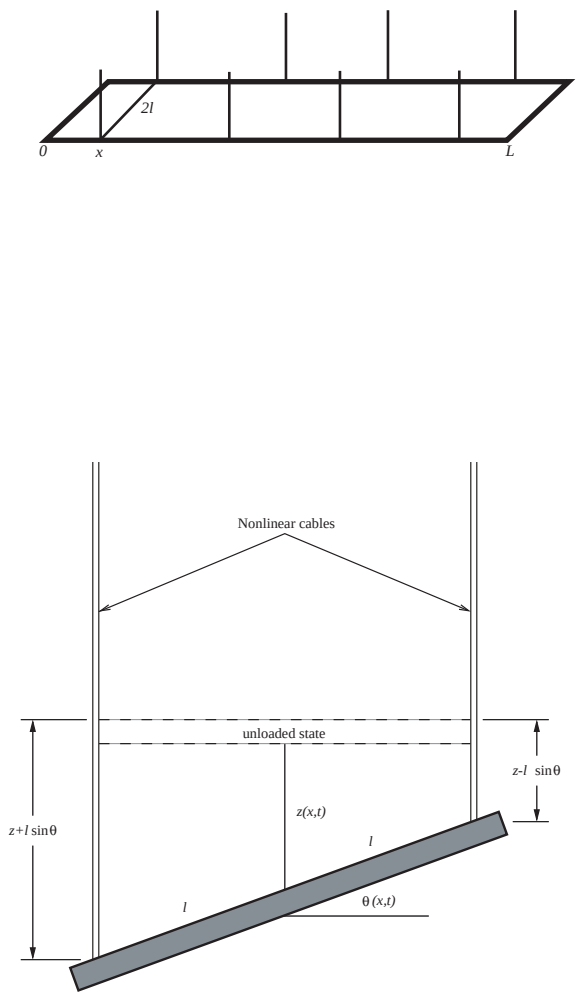

Figure 1: A simple model of the center span and its horizontal cross section

where $u^+ = \max\{u, 0\}$. The force exerted by the left hand cable can be described analogously (using $z + l\sin\theta$ instead of $z - l\sin\theta$).

Using Newton's second law, the torsional and vertical motions are governed by

$$\left\{ \begin{array}{c} \theta'' = \frac{3K}{ml}\cos\theta[(z - l\sin\theta)^+ - (z + l\sin\theta)^+] - \delta_1\theta' + \lambda_T\sin(\mu_T t) \\ z'' = -\frac{K}{m}[(z - l\sin\theta)^+ + (z + l\sin\theta)^+] - \delta_2 z' + g + \lambda_V\sin(\mu_V t) \\ \theta(0) = \theta_0, \theta'(0) = \theta_0', z(0) = z_0, z'(0) = z_0' \end{array} \right\}. \quad (1)$$

Here K is the Hooke's Law spring constant of the cables, m is the mass per unit length of the roadbed, δ_1 and δ_2 are damping constants, λ_T, μ_T are the amplitude and frequency of the external torsional forcing, λ_V, μ_V are the amplitude and frequency of the external vertical forcing, and $g \approx 10$ is the gravitational acceleration. The derivation of this model and justification of the sinusoidal external forcing are discussed in [7], [9].

Remark 2.1 *Observe that if the cables never slacken, i.e., if $z \pm l\sin\theta \geq 0$ and hence $(z \pm l\sin\theta)^+ = z \pm l\sin\theta$, the system (1) becomes uncoupled, yielding the single equations*

$$\theta'' = -\frac{6K}{m}\cos\theta\sin\theta - \delta_1\theta' + \lambda_T\sin(\mu_T t) \quad (2)$$

$$z'' = -\frac{2K}{m}z - \delta_2 z' + g + \lambda_V\sin(\mu_V t). \quad (3)$$

Observe that (2) is the forced, damped pendulum equation, which is known to have chaotic solutions, [4]. The structure of the set of periodic solutions to the single equation (2) was studied in [8], [10], [11].

Since the decoupling of the equations described above holds unless $z \pm l\sin\theta < 0$, the nonlinear effects in the vertical equation do not come into play before one side of the span is deflected upward by about 12 meters.

2.2 A smoothed version of the system (1)

In this section we construct a smoother version of (1) so that the nonlinearity comes into play for smaller upward deflections (see remark 2.1 above). We want a nonlinearity that remains approximately linear over several meters, stiffens somewhat as the downward deflections go beyond that, and weakens slightly as the upward deflections exceed that linear range.

A caution is in order at this point: we now change our choice of coordinates so that the equilibrium is chosen as the origin, unlike the earlier equation (1) where the origin was the unloaded state. We let $y(t)$ be the downward displacement of the center of the cross section from equilibrium at time t.

In [9], the authors smoothed the nonlinear terms in (1); more specifically, they considered a cable force of the form

$$f(u) = -\frac{1}{a}(e^{au} - 1) \tag{4}$$

where u is the stretch in the cable from equilibrium. Figure 2 shows the force due to the cables as a function of the stretch in the cable (i.e., $f(u)$ versus u) under our two different assumptions: the piecewise linear cable described in section 2.1 and the smooth nonlinear cable described in (4). How nonlinear the system is depends on the coefficient a: the smaller a is, the closer to linear the system is in a range about equilibrium. As discussed below, we shall take a to be quite small.

As we noted in section 1, this second assumption more realistically captures the qualitative behavior of the cables; the cables resist elongation linearly near equilibrium, superlinearly for large displacements, and exert small nonzero resistance to compression. Moreover, it was shown in [9] and we will demonstrate further in section 4 that the solutions to the resulting coupled system,

$$\left\{ \begin{array}{c} \theta'' = \frac{3K}{ml}\cos\theta[\frac{1}{a}e^{a(y-l\sin\theta)} - \frac{1}{a}e^{a(y+l\sin\theta)}] - \delta_1\theta' + \lambda_T\sin(\mu_T t) \\ y'' = -\frac{K}{m}[\frac{1}{a}(e^{a(y-l\sin\theta)} + e^{a(y+l\sin\theta)} - 2)] - \delta_2 y' + \lambda_V\sin(\mu_V t) \\ \theta(0) = \theta_0, \theta'(0) = \theta_0', y(0) = y_0, y'(0) = y_0' \end{array} \right\} \tag{5}$$

more accurately replicate the phenomena observed at Tacoma Narrows on the day of its collapse.

2.3 The Choice of Physical Parameters

In solving (1) and (5) numerically, we choose the physical constants $K = 1000, m = 2500, l = 6$, and $\delta_1 = \delta_2 = 0.1$ in accordance with the historical data on the Tacoma Narrows Bridge, [2]. We choose $a = 0.1$ so that the restoring force due to the cables is approximately linear near equilibrium; see

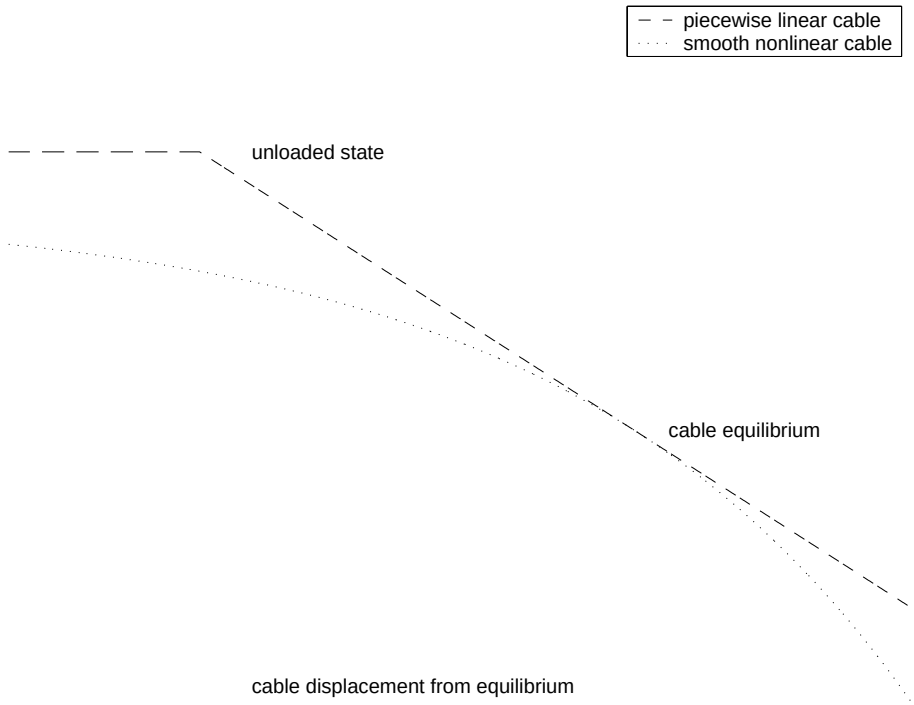

Figure 2: Two different models of the cable force

figure 2. Observe that in (5), as the displacements $y \pm l \sin\theta$ become large and negative (i.e., when the cable slackens), the first term in the equation for the vertical motion approaches $\frac{2K}{ma} = \frac{2 \cdot 1000}{2500 \cdot 0.1} = 8 \approx g$, the acceleration due to gravity.

We choose the torsional and vertical forcing frequencies μ_T and μ_V to approximate the frequencies of the oscillations observed at Tacoma Narrows on the day of its collapse, which were approximately 14 cycles per minute and 38 cycles per minute for the torsional and vertical motions, respectively. These values correspond to $\mu_T \approx 1.5$ and $\mu_V \approx 4.0$. We studied values of $\mu_T \in (0.8, 1.6)$ and $\mu_V \in (1.6, 5.2)$. Note that the resonant frequencies for the linearized ODEs are $\mu_T^R \approx 1.5$ and $\mu_V^R \approx 0.9$.

Since we wish to find periodic solutions (θ, y) and (θ, z) to the coupled systems (1) and (5), respectively, we choose the frequencies so that $\mu_V = N\mu_T$. Note that the frequency ratio $N = \frac{\mu_V}{\mu_T}$ observed at Tacoma Narrows was $N \approx \frac{4}{1.5} = 2.7$.

3 Results for the Piecewise Linear Model

In this section, we briefly describe our results on large torsional and periodic solutions to (1). We reiterate first that the phenomena that we wish to replicate are a rapid transition to large torsional motion or large periodic torsional motion in the presence of small vertical oscillation and little or no torsional forcing.

To investigate the solutions to (1), we specified the initial values θ_0, θ_0', z_0, z_0' and the forcing parameters λ_T,μ_T, λ_V, μ_V, numerically solved the initial value problem (1) using a second order Runge-Kutta method, and examined the short and long term behavior of the solution.

We found that although we can replicate the desired transition to torsional motion, unreasonably large initial vertical displacements are required to do so. For example, figure 3 shows that when $\lambda_T = 0.04$, $\mu_T = 1.2$, $\lambda_V = 4$, $\mu_V = 2.4$, an initial vertical displacement of 28 meters (15.5 meters from the equilibrium solution $(\theta, z) = (0, 12.5)$) is required to induce torsional oscillation of about 1 radian. This was the case over the range of amplitudes and frequencies λ_T,μ_T, λ_V, μ_V that we tested; unreasonably large vertical impulses were required to replicate the desired phenomenon. Figure 4 shows the short and long term torsional behavior of this solution in which the large

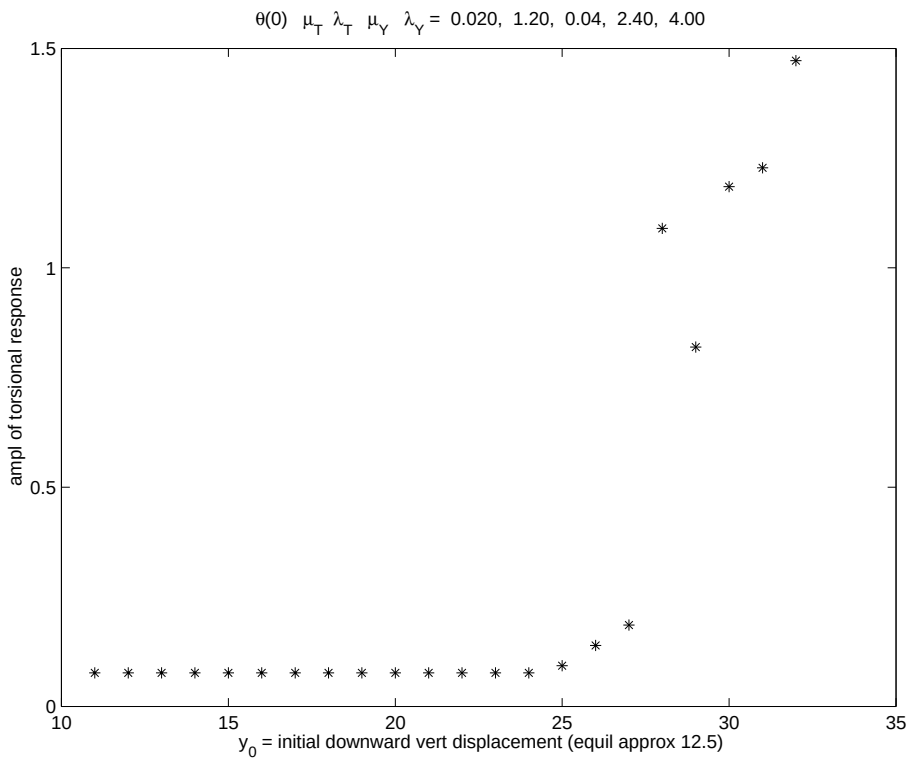

Figure 3: To induce large torsional motion, we must impose unreasonably large vertical initial displacement.

vertical motion induces a large torsional response.

In the next section, we improve this result considerably; we find that in the smoothed model, for the same values of μ_T and μ_V, small vertical oscillation is sufficient to induce and sustain large torsional motion, even with zero torsional forcing.

In addition to the results described above, we employed a more systematic study of the periodic solutions to (1) via numerical continuation algorithms, which are described in [10]. However, we did not find periodic solutions to the fully coupled system; the family of periodic solutions that we were able to find via numerical continuation on (1) were solutions to the *uncoupled* system described in remark 2.1; i.e., in the periodic solutions that we found, the vertical deflections were sufficiently small so that $z \pm l \sin\theta \geq 0$ and the equations remained uncoupled. The structure of the set of periodic solutions

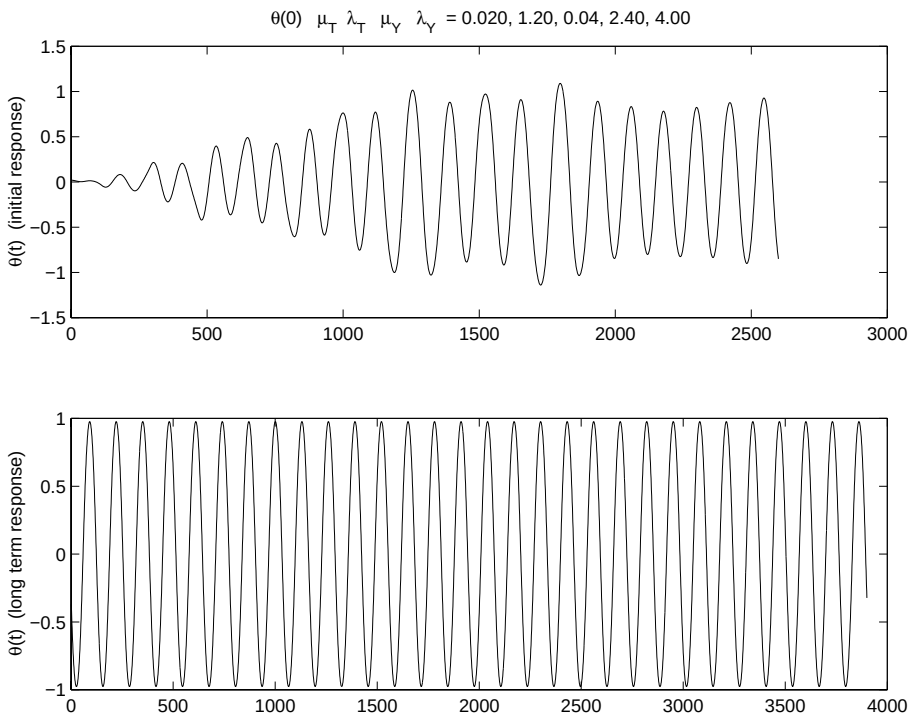

Figure 4: A solution in which a large vertical impulse ($z_0 = 28$) induces a rapid transition to large torsional oscillation. These solutions were first presented in [7].

to the equation (2) is described in [8] and [10].

Doole and Hogan first studied the bifurcation and stability properties of periodic solutions to systems of the form (1) in [5] for a slightly smoother nonlinearity and with $\mu_T = \mu_V$. The coefficients $\frac{3K}{ml}$ and $\frac{K}{m}$ of the nonlinear terms differ considerably. In this paper, they demonstrated the existence of multiple periodic solutions, period-doubling sequences and the onset of 'beats' via torus bifurcations.

4 Bifurcation and Stability Results for the Smoothed Model

In this section, we describe the bifurcation and stability properties of periodic solutions to the smoothed coupled system (5). In each experiment that follows, we fix μ_T, μ_V, λ_V and employ pseudo-arclength continuation to examine how the amplitudes a_T and a_V of the periodic torsional and vertical responses change as we vary the torsional forcing amplitude λ_T.

Pseudo-arclength continuation is described in more detail in [8], [10]. A brief description of the algorithm is as follows. Fix λ_T small and take a "good guess" at initial conditions $\theta_0, \theta_0', y_0, y_0'$ that yield a τ periodic solution to (5). Solve the initial value problem (5) for $t \in (0, \tau]$. If the resulting solution is indeed periodic, record its amplitude $a = (a_T, a_V)$, increment λ_T, and repeat. If the computed solution is not periodic, update the initial guess via Newton's method and try again. We encounter difficulties when the Jacobian used in the Newton update becomes singular. This occurs exactly at bifurcation points, but we avoid this problem via pseudo-arclength parameterization, [6].

We also examined the stability of our computed periodic solutions via the usual method: we linearized the system (5) about the computed periodic solution and examined the magnitude of the eigenvalues of the matrix $\Phi(\tau)$, the fundamental solution to the linearized system, [3].

In the experiments that follow, we study $a = (a_T, a_V)$ versus λ_T for several different values of $\mu = (\mu_T, \mu_V)$. In each case, we compute the vertical forcing amplitude λ_V to induce small vertical oscillation; more specifically, we compute λ_V so that the forced response in the linearized vertical equation will have amplitude of less than one meter.

The central theme of these experiments is that even quite small vertical forcing term λ_V can induce a large torsional subharmonic response.

4.1 Bifurcation curves for N=2

In this section, we study the dependence of the torsional and vertical amplitudes of the resulting periodic solutions $a = (a_T, a_V)$ on the size of the forcing term λ_T when the frequency of the vertical forcing term μ_V is twice that of the torsional frequency μ_T.

Experiment 1: $\mu = (\mu_T, \mu_V) = (1, 2)$
We begin with a classic example of our main conclusion in the first experiment. Figure 5 summarizes the results; the top graph shows a_T versus λ_T and the middle graph shows a_V versus λ_T. The third graph shows a close-up of the top graph near $\lambda_T = 0$. The vertical forcing amplitude λ_V , which remains constant for the course of the continuation, is chosen to give a vertical displacement of approximately 0.2 meters. As we start increasing λ_T, the vertical oscillation remains uncoupled and constant as the torsional oscillation increases approximately linearly. When $\lambda_T \approx .59$, we reach a turning point in the torsional amplitude a_T and we eventually double back across the $\lambda_T = 0$ axis.

These points on the curve best illustrate our conclusion. The same vertical forcing term that will induce a small vertical oscillation of approximately 0.2 meters can also sustain a subharmonic motion of approximately the same small vertical amplitude, but with a torsional component of approximately 1.2 radians, which would correspond to a vertical motion at the side of approximately 7 meters.

We also note the following:

1. When $\lambda_T \in [0, 0.59]$, there are three periodic solutions to (5), one of small amplitude and two of large (torsional) amplitude.

2. The solutions along the bottom branch and the beginning of the top branch of the curve are stable, while the solutions on the middle branch are unstable, as are the solutions along the top branch for large λ_T. Observe though that the values of λ_T that correspond to these top branch unstable solutions are physically unreasonable.

3. When $\lambda_T = 0$, there are two solutions of large (torsional) amplitude. Since there is no torsional forcing present, it is the vertical motion alone that is sustaining the torsional oscillation. Moreover, the vertical oscillation is less than half a meter in amplitude. This is one of our main results: *small vertical motion can induce and sustain large torsional motion, even in the absence of torsional forcing.* This was not the case for the piecewise linear model (1). Figure 6 shows $\theta(t)$ and $y(t)$ versus t for one of the solutions along the top branch of the bifurcation curve very close to $\lambda_T = 0$. The solution that we selected is indicated on the third graph in figure 5.

4. The qualitative properties of the oscillation, namely vertical oscillation of less than one meter and torsional oscillation of approximately one radian, are consistent with the behavior observed at Tacoma Narrows on the day of its collapse, [2].

Experiment 2: $\mu = (1.2, 2.4)$ and $\mu = (1.4, 2.8)$
The results for these values of μ are consistent with the phenomena described in items 1 through 4 above. Figure 7 shows the bifurcation curves a_T versus λ_T and a_V versus λ_T for $\mu = (1.2, 2.4)$. We note that the amplitude of the vertical motion is larger than in Experiment 1, but is still considerably less than one meter. Also, the amplitude of the torsional motion when $\lambda_T = 0$ has decreased from that in Experiment 1, but it is still close to one radian.

Experiment 3: $\mu_T > \mu_T^R$, $\mu = (1.6, 3.2)$
Figure 8 shows that when the torsional forcing frequency μ_T exceeds the resonant frequency $\mu_T^R \approx 1.55$, we do not find multiple periodic solutions for fixed λ_T; instead a_T increases with λ_T. This is consistent with our results in [8], [10], [11] for the single torsional equation (2). Here we found that if $\mu_T < \mu_T^R$, the a_T versus λ_T curve is S-shaped as in figure 7, but if $\mu_T > \mu_T^R$, the curve has the shape shown in figure 8. These are the only shapes that can arise for the single equation, since we are examining one response (a_T) against two control parameters (λ_T and μ_T). In this paper we are studying two responses (a_T and a_V) as we vary four control parameters ($\lambda_T, \mu_T, \lambda_V$, and μ_V), thus we expect more complicated surfaces similar to those that arise in catastrophe theory, [13]. We are only able to show two-dimensional cross-sections of higher-dimensional surfaces. Nonetheless, the curves shown

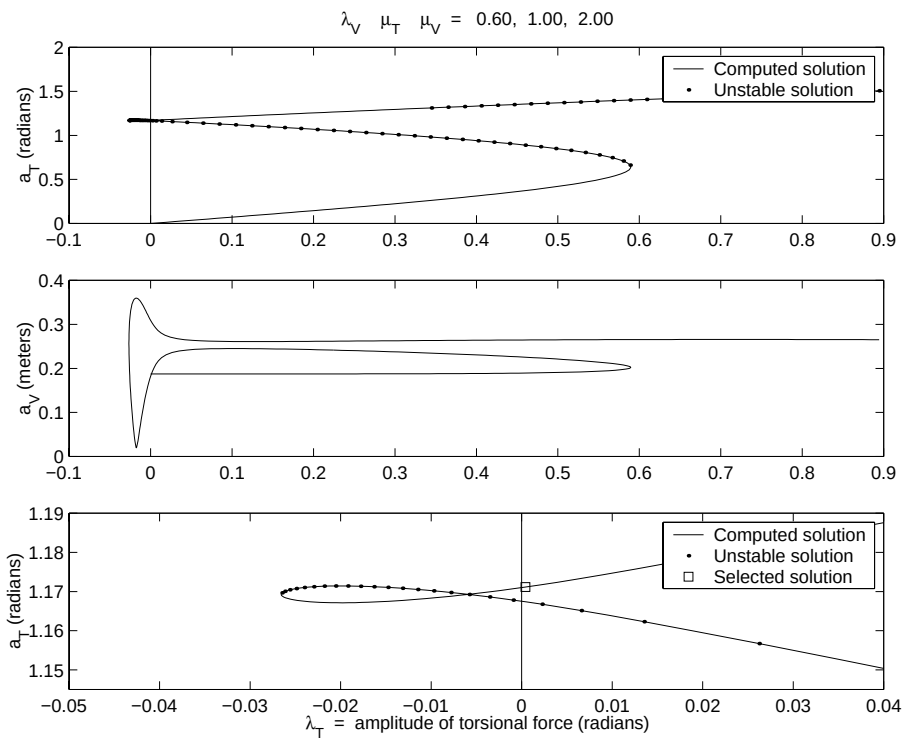

Figure 5: Experiment 1. $(\mu_T, \mu_V) = (1.0, 2.0)$ Initially, vertical forcing is uncoupled from the torsional. After the turning point, the subharmonic torsional motion crosses the $\lambda_T = 0$ axis, giving a motion that is primarily subharmonic and torsional, with only vertical forcing.

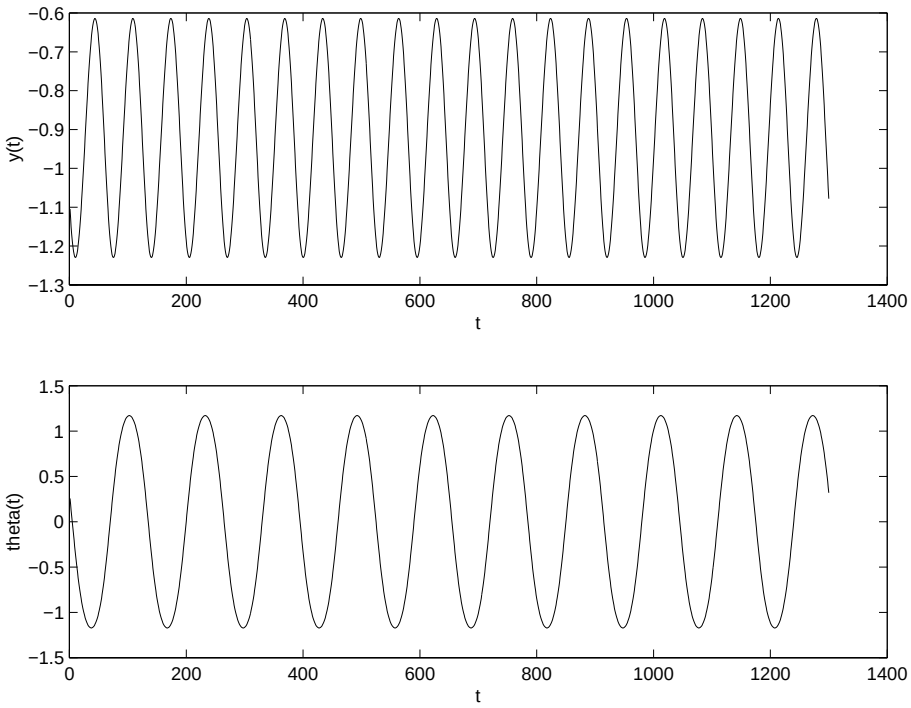

Figure 6: Experiment 1. The details of the solution in which small vertical forcing is sufficient to sustain large torsional motion, even in the absence of torsional forcing. Note how the oscillation is centered about 1 meter above the equilibrium $y = 0$. This indicates that the center span of the bridge is raised; this actually happened in the Tacoma Narrows collapse.

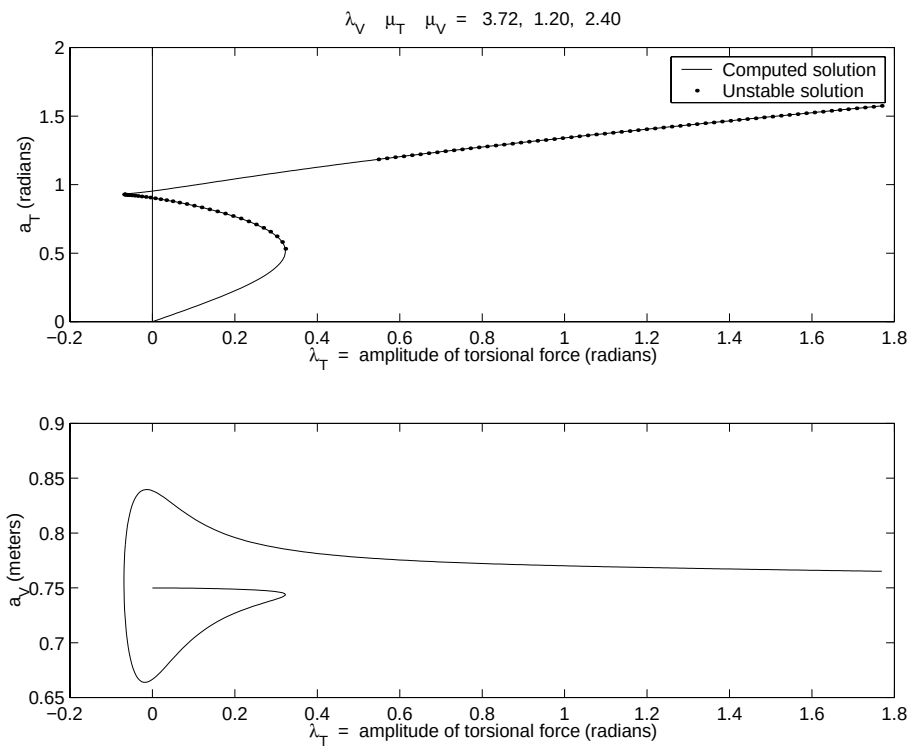

Figure 7: Experiment 2. $(\mu_T, \mu_V) = (1.2, 2.4)$ The same phenomenon as in Experiment 1, for an increased frequency, indicating that the phenomenon occurs over a range of frequencies.

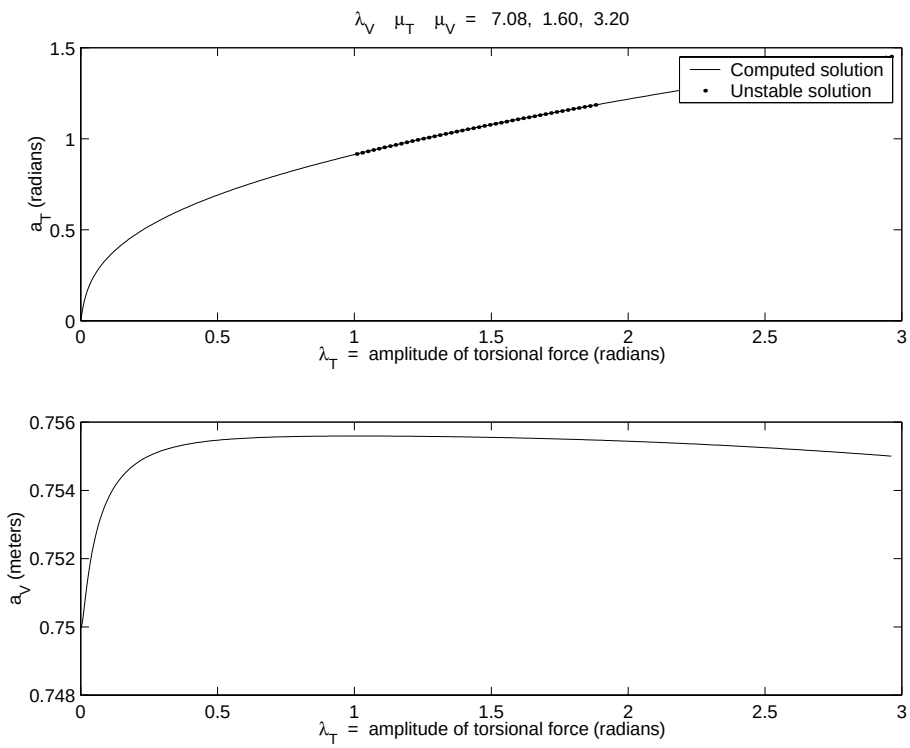

Figure 8: Experiment 3. $(\mu_T, \mu_V) = (1.6, 3.2)$. As the torsional frequency is increased above the torsional resonant frequency, the turning point disappears and we lose the existence of multiple solutions.

in figure 5 and the figures that follow are strikingly reminiscent of the cross-sections of the parabolic umbilic surfaces of [13].

Experiment 4: $\mu_V \approx 2\mu_V^R$; $\mu = (0.9, 1.8)$
Figure 9 shows that when the vertical forcing frequency is close to double the resonant frequency $\mu_V^R \approx 0.89$, the bifurcation curve has a very different shape. Small vertical forcing (λ_V inducing a vertical oscillation in the linear range of about 1 meter) can also induce large subharmonic vertical oscillation ($a_V \geq 5$ meters). Also, we do not find large torsional periodic solutions for small λ_T.

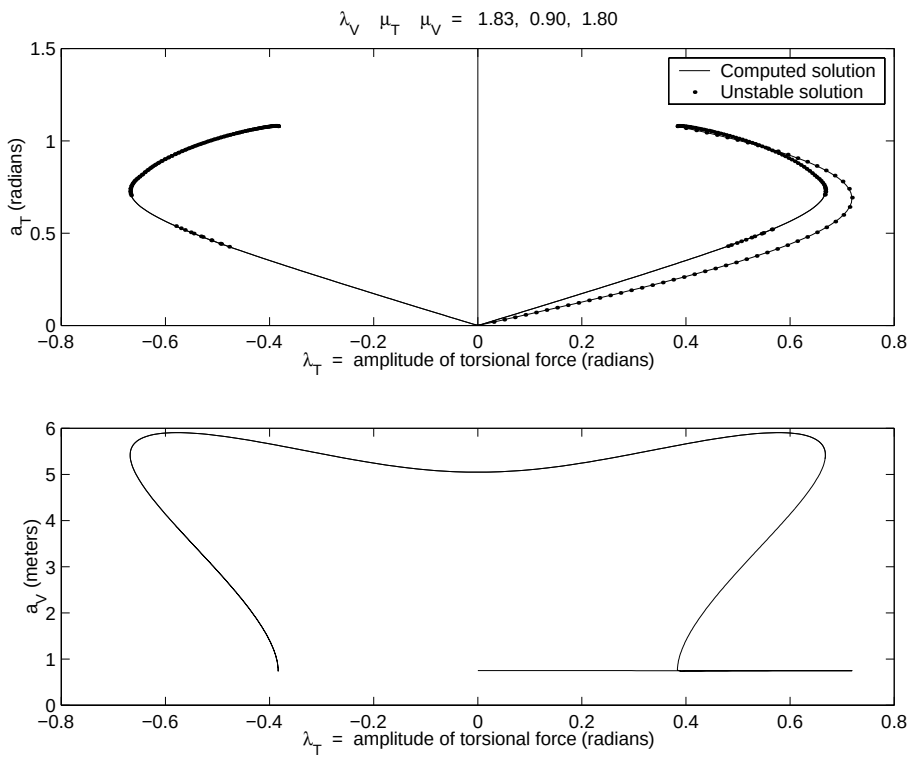

Figure 9: Experiment 4. $(\mu_T, \mu_V) = (0.9, 1.8)$ In this range of frequency, with the vertical forcing near double the vertical resonant frequency, subharmonic large amplitude vertical solutions exist along with the smaller amplitude (approx. 1 meter) solutions on the lower branch. Note the changes in stability properties along the torsional branch, indicating that period-doubling may be occurring.

4.2 Bifurcation curves for N=4

In this section, we study the dependence of $a = (a_T, a_V)$ on λ_T when $\mu_V = 4\mu_T$. Since our results are consistent with those discussed in section 4.1, we describe them briefly and show only a few figures.

Experiment 5: $\mu = (1.0, 4.0), \mu = (1.1, 4.4), \mu = (1.2, 4.8)$.

For μ in this range ($\mu_V > \mu_V^R$ and $\mu_T < \mu_T^R$), the bifurcation curves a_T versus λ_T are S-shaped and cross the vertical axis near $a_T = 1$, corresponding to large torsional motion in the absence of torsional forcing. Moreover, the vertical oscillation that sustains this torsional motion is less than one meter in amplitude. The solutions on the middle branch are unstable while the solutions on the bottom and top branches are stable (except for unreasonably large λ_T). Figure 10 shows the bifurcation curves for $\mu = (1.1, 4.4)$.

The graphs in the right-hand column of figure 10 show close-ups of the bifurcation curves in the left-hand columns. We observe a complicated "bowtie" in the curve near $\lambda_T = 0$ with interesting stability changes; again, these curves are reminiscent of the cross sections shown in [13]. This occurred in our other experiments with $N = 4$; there are similar "bowties" in the curves for $\mu = (1.0, 4.0)$ and $\mu = (1.2, 4.8)$. The behavior near $\lambda_T = 0$ was less complicated when $N = 2$; see figures 5 and 7.

Experiment 6: $\mu_V \approx 4\mu_V^R$

When μ_V is close to four times the resonant frequency μ_V^R, the bifurcation curve is similar to the one shown in figure 9; we do not show it here.

4.3 Bifurcation curves for N=3

In this section, we study the dependence of $a = (a_T, a_V)$ on λ_T when $\mu_V = 3\mu_T$. Our results differ considerably from those presented in sections 4.1 and 4.2.

Experiment 7: $\mu_V > \mu_V^R$ and $\mu_T < \mu_T^R$

Figures 11 and 12 show the bifurcation curves when $\mu = (1, 3)$ and $\mu = (1.3, 3.9)$. In both cases we note the following.

1. The curve a_T versus λ_T is S-shaped, as in sections 4.1 and 4.2, but we do not find large amplitude torsional oscillation corresponding to $\lambda_T = 0$; i.e., the a_T versus λ_T curve does *not* cross the vertical axis as it did when $N = 2, N = 4$ for μ in this range. Thus, we cannot induce

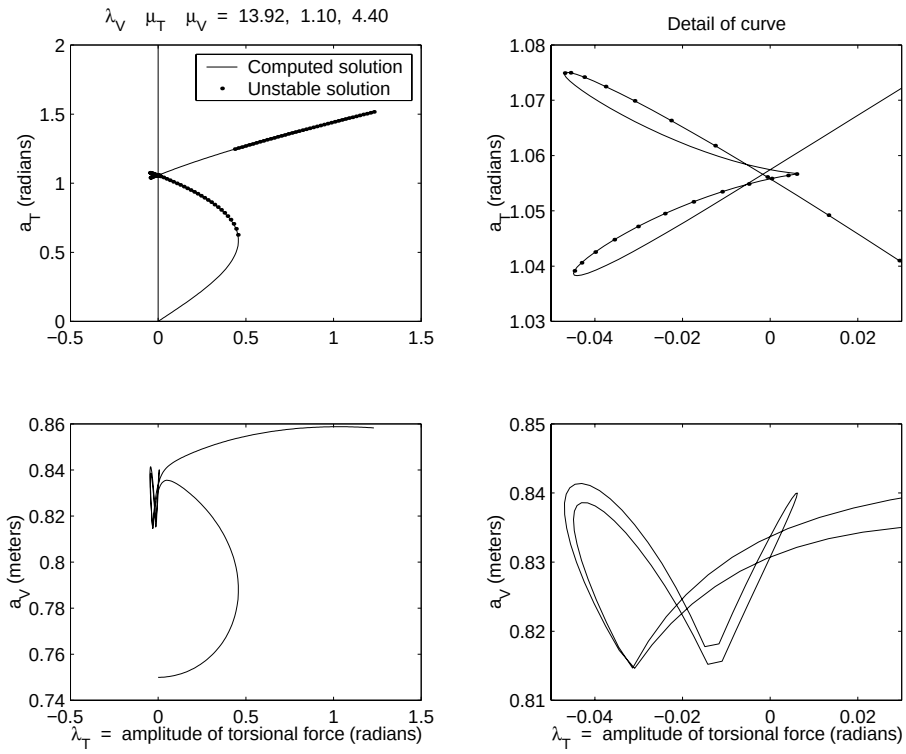

Figure 10: Experiment 5. $(\mu_T, \mu_V) = (1.1, 4.4)$ Similar results to Figures 5 and 7, with a torsional response of four times the period of the vertical forcing.

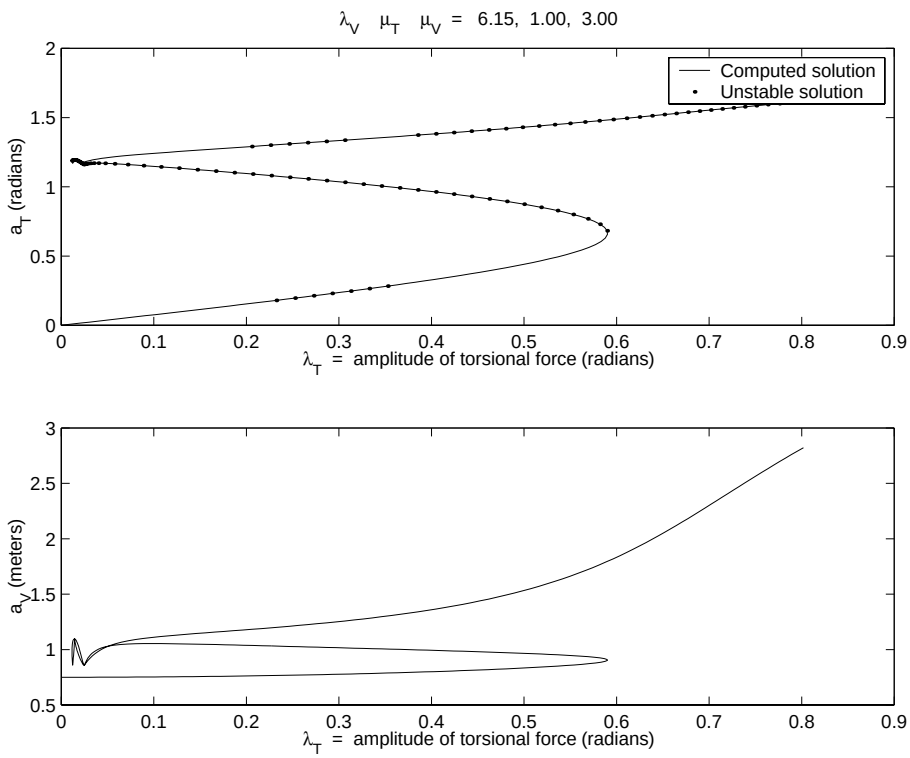

Figure 11: Experiment 7. $(\mu_T, \mu_V) = (1.0, 3.0)$ We fail to pick up solutions with large torsional component and zero torsional forcing. Some tiny torsional forcing is still apparently necessary to maintain torsional motions.

large torsional motion without imposing some torsional forcing when $N = 3$.

2. The graphs in the right-hand column of figure 12 show close-ups of the bifurcation curves pictured in the left-hand column. The curves are less complicated than when $N = 4$, but more complicated than when $N = 2$ (see figures 5, 10).

3. The slope of the a_V versus λ_T curve is large for large λ_T. This did not occur for $N = 2$ or $N = 4$; for example, see figures 7, 10.

Experiment 8: $\mu_V \approx 3\mu_V^R$; $\mu = (0.87, 2.6)$
Figure 13 shows that when the vertical forcing frequency is approximately

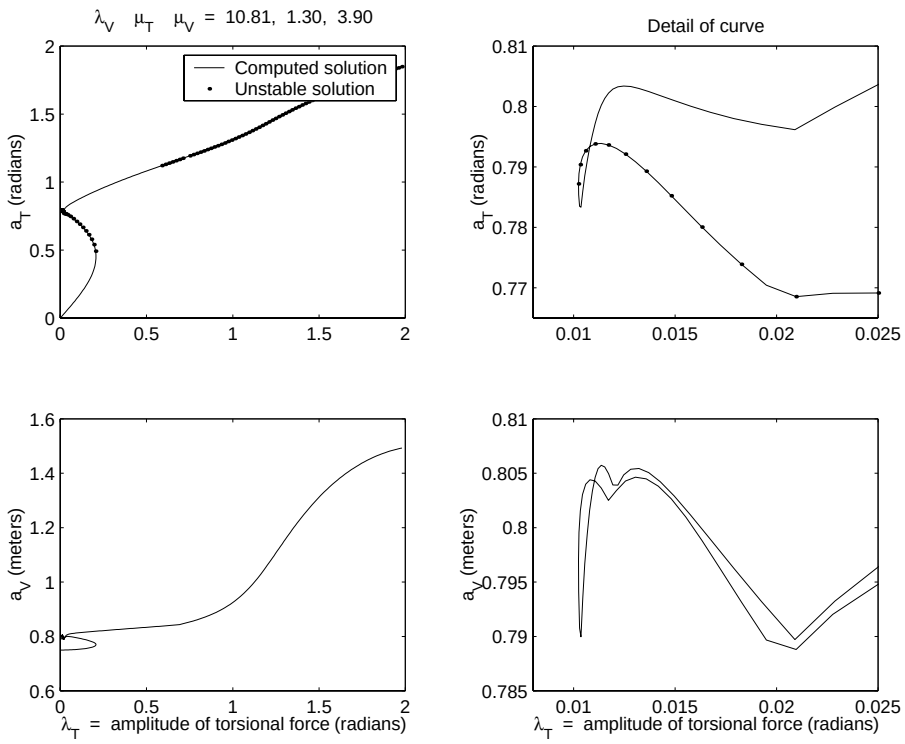

Figure 12: Experiment 7. $(\mu_T, \mu_V) = (1.3, 3.9)$

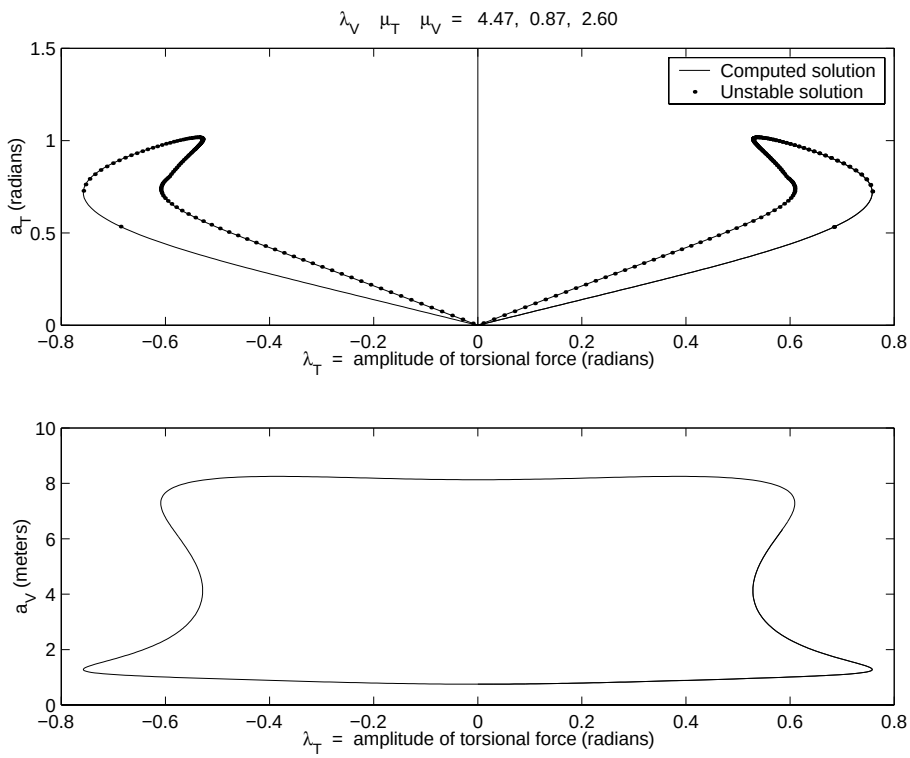

Figure 13: Experiment 8. A closed, symmetric bifurcation curve with unstable solutions of small torsional amplitude.

three times the vertical resonant frequency, the bifurcation curves are closed and symmetric. This is similar to our results for $N = 2$ and $N = 4$.

4.4 Bifurcation curves for N=2.5

We will now discuss what may be the most dramatic result of this paper. It is motivated by the historical accounts of the collapse of the Tacoma Narrows bridge. In that case, the bridge was oscillating vertically and then switched almost instantaneously into a primarily torsional oscillation; the frequency of the initial vertical oscillation was about 2.7 times that of the torsional oscillation.

In Experiments 1-3,5, and 7, we found only *stable* small amplitude solutions. In Experiments 4, 6 and 8, we found unstable solutions of small torsional amplitude, but they did not grow to large torsional oscillation. So

far, unstable solutions of small torsional amplitude that grow to large torsional motion have eluded us. We demonstrate their existence in this section. It is remarkable that we found this phenomenon only for $N = 2.5$, which is close to the frequency ratio observed at Tacoma Narrows on the day of its collapse ($N \approx 2.7$).

Experiment 9: $\mu_V = 2.5\mu_T$

In this experiment we take $\mu_T = 1.2, \mu_V = 3.0$. To model the scenario at Tacoma Narrows described above, we fixed a vertical forcing term whose amplitude keeps us in the close-to-linear range of about 1.5 meters. Note that the periods of the torsional and vertical forcing are $\tau_T = \frac{2\pi}{\mu_T}$ and $\tau_V = \frac{2\pi}{\mu_V} = \frac{2\pi}{2.5\mu_T}$, respectively. Figure 14 shows the bifurcation curve of periodic solutions with period $\tau = 2\tau_T = 5\tau_V$; this contains a major new finding. The lower branch, which was in approximately linear range has now become unstable, with very small torsional forcing.

Figure 15 shows the short and long term torsional response for one unstable periodic solution along the bottom branch of the bifurcation curve from figure 14. Observe that initially, the torsional amplitude is small (≈ 0.01 radians), but over time it grows to large torsional oscillation (≈ 0.62 radians). Note also that the period of the motion has quadrupled.

Figure 16 shows the corresponding vertical response. We see that the amplitude of the vertical motion does not change over time; it remains fixed at less than two meters. However, the period of the motion has increased by a factor of twenty.

Note that the unstable bottom branch solution did not approach the stable top branch solution "above" it on the bifurcation curve, whose torsional amplitude is approximately one radian. Rather, it settled down to some other stable periodic solution that is not shown on the curve.

5 Concluding Remarks and Open Questions

As these results (and the Millennium Bridge experience) suggest, much of the dynamics of the away-from-equilibrium motions of large suspended beams or plates remains unexplored, with many counter-intuitive results presumably still to be discovered.

In particular, very mild coupling in the vertical and torsional oscillations can result in purely vertical forcing creating large amplitude torsional mo-

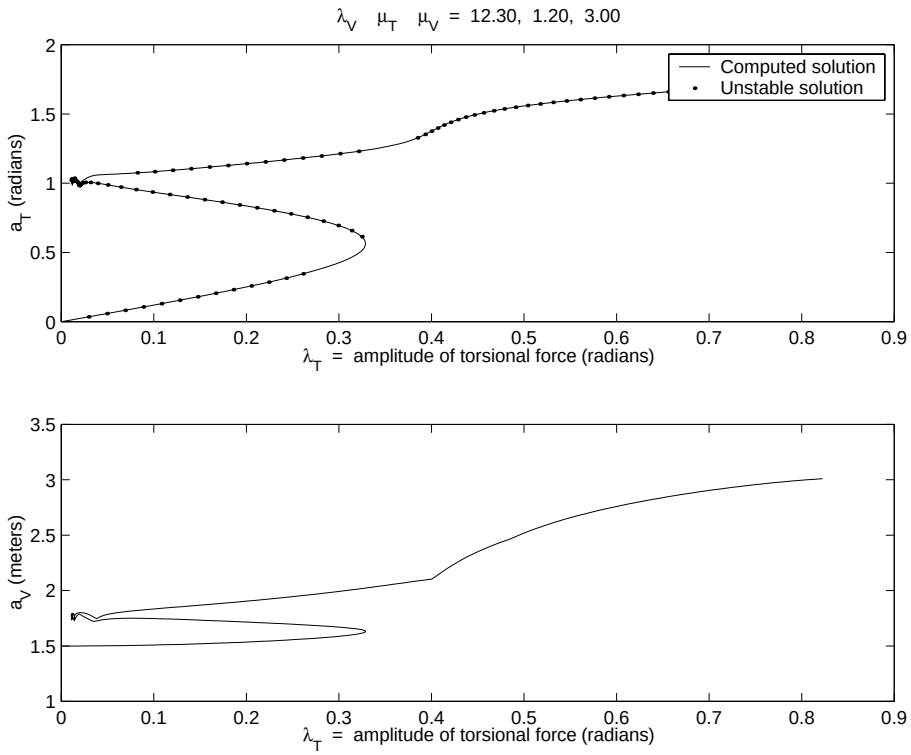

Figure 14: Experiment 9. We find unstable solutions of small torsional amplitude when N=2.5

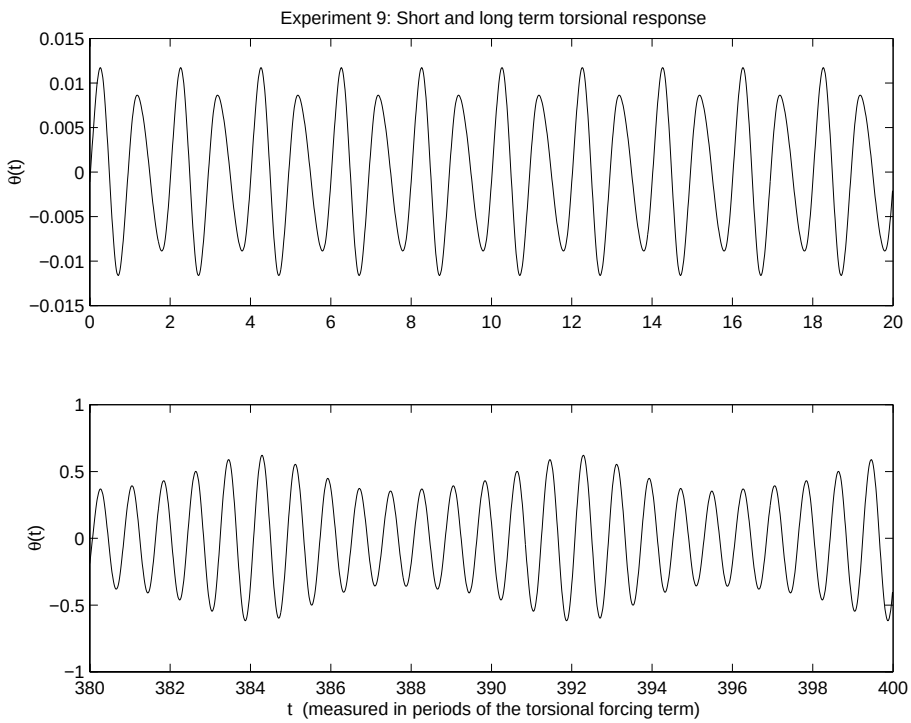

Figure 15: Experiment 9. The short and long term torsional response for an unstable periodic solution. Over time, the amplitude of the oscillation increases dramatically and the period quadruples.

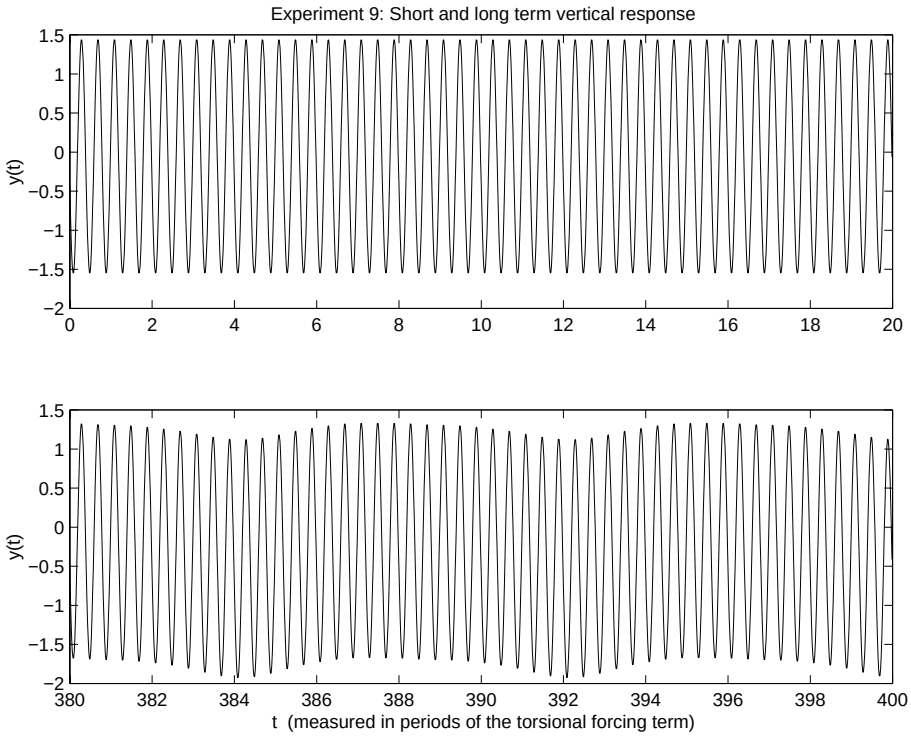

Figure 16: Experiment 9. The short and long term vertical response for an unstable periodic solution.

tions. We have not addressed the question of allowing lateral motions to be coupled with both of these. (Partly, this was because there were no significant lateral motions in the Tacoma Narrows bridge, which was the source of most of our physical data and the origin of our choices of constants.)

Presumably, an improved understanding of all three degrees of freedom will eventually lead to a better understanding of away-from-equilibrium motions such as those on the Millennium Bridge as well as ways of avoiding them.

Our results in sections 3 and 4 introduce several open questions. Some of these are listed below.

- In section 4, we demonstrated numerically the existence of multiple periodic solutions to the system (5). Can we prove their existence analytically? (Existence and multiplicity theorems for piecewise linear PDE systems of the form (1) were established in [10],[11].)

- The bifurcation curves cross the vertical axis when $N = 2$ and $N = 4$, but not when $N = 3$. Is there a mathematical explanation for this? Is there a physical explanation?

- Our results in section 4.4 demonstrate that there are other periodic solutions besides the ones that we found via continuation. How can we find these other solutions? What are their qualitative properties?

This last question highlights both the challenge and the danger of mathematical modeling in nonlinear dynamics. When studying a system with solely vertical forcing, one must impose some simplifications. The most natural temptation would be to study the vertical ordinary differential equation without studying the torsional degree of freedom. This would, of course, have resulted in neglecting some of the most important aspects of the problem.

Finding large torsional responses from the purely vertical forcing was basically an accident. Is there a scientific way to discover the periodic solutions that are 'out there' in infinite-dimensional space, some of which might have even three degrees of freedom? Global methods of finding large amplitude periodic solutions are limited to a few methods such as continuation and mountain pass algorithms. Finding more reliable methods may well be one of the challenges of the next century.

References

[1] F.E. Allen. *London bridge is falling down.* American Heritage, **51** (2000), no. 6, p. 19.

[2] O.H. Amann, T. von Kármán, and G.B. Woodruff. *The Failure of the Tacoma Narrows Bridge.* Federal Works Agency, 1941.

[3] E.A. Coddington and N. Levinson. *Theory of Ordinary Differential Equations.* McGraw-Hill, New York, 1955.

[4] Blanchard, Devaney, and Hall. *Differential Equations.* Brooks/Cole Publishing Company, Pacific Grove, 1998.

[5] S.H. Doole and S.J. Hogan. *Non-linear dynamics of the extended Lazer-McKenna bridge oscillation model.* Dyn. Stab. Syst., **15** (2000), no. 1 43–58.

[6] H. B. Keller. *Lectures on Numerical Methods in Bifurcation Problems.* Springer-Verlag, Berlin, 1987.

[7] P.J. McKenna. *Large torsional oscillations in suspension bridges revisited: fixing an old approximation.* Amer. Math. Monthly, **106** (1999), no. 1, 1–18.

[8] P.J. McKenna and K.S. Moore. *Multiple periodic solutions to a suspension bridge ordinary differential equation.* Electron. J. Differ. Equ. Conf., 5 (2000) 183–199.

[9] P.J. McKenna and Cilliam O'Tuama. *Large torsional oscillations in suspension bridges visited again: vertical forcing creates torsional response.* Amer. Math. Monthly, **108** (2001), no. 8, 738–745.

[10] K.S. Moore. *Large amplitude torsional oscillations in a nonlinearly suspended beam: a theoretical and numerical investigation.* Dissertation, University of Connecticut, 1999.

[11] K.S. Moore. *Large Torsional Oscillations in a Suspension Bridge: Multiple Periodic Solutions to a Nonlinear Wave Equation.* SIAM J. Math. Anal., to appear.

[12] R.H. Scanlan and J.J. Tomko. *Airfoil and bridge deck flutter derivatives.* Proc. Am. Soc. Civ. Eng. Eng. Mech. Division, EM6, 1717-1737, 1971.

[13] E. C. Zeeman. Catastrophe theory. Selected papers, 1972-1977. Addison-Wesley, London, 1977.